SCIENCE CHINA
Technological Sciences

September 2013 Vol.56 No.9: 2170–2177
doi: 10.1007/s11431-013-5313-3

On the nature of tip clearance flow in subsonic centrifugal impellers

LIU ZhengXian[1, 2*], PING Yan[1] & ZANGENEH Mehrdad[3]

[1] *School of Mechanical Engineering, Tianjin University, Tianjin 300072, China;*
[2] *State Key Laboratory of Engines, Tianjin University, Tianjin 300072, China;*
[3] *Department of Mechanical Engineering, University College London, London WC1E 6BT, UK*

Received June 6, 2013; accepted July 16, 2013

Increasing demand for downsizing of engines to improve CO_2 emissions has resulted in renewed efforts to improve the efficiency and expend the stable operating range of the centrifugal compressors used in petro-chemical equipment and turbochargers. The losses in these compressors are dominated by tip clearance flow. In this paper, the tip clearance flow in the subsonic impeller is numerically investigated. The nature of the tip clearance in inducer, axial to radial bend and exducer are studied in detail at design and off-design conditions by examining the detailed flow field through the clearance and the interaction of the clearance flow with the shear effect with the endwalls. The correlation between blade loading and span wise geometry and clearance flow at different locations are presented.

centrifugal impeller, tip clearance, subsonic flow, numerical simulation, blade loading

Citation: Liu Z X, Ping Y, Zangeneh M. On the nature of tip clearance flow in subsonic centrifugal impellers. Sci China Tech Sci, 2013, 56: 2170–2177, doi: 10.1007/s11431-013-5313-3

1 Introduction

Impeller tip clearance has a major influence on losses and stability of centrifugal compressors. Specifically, the interaction of tip leakage flow with secondary flows and inducer shockwaves in the transonic impellers has a major impact on losses within the impeller and the flow field of impeller exit. The effect of clearance losses becomes increasingly more significant as exit blade width is reduced. The pressure to cut CO_2 emissions and the resulting downsizing of petrol and diesel engines has meant that smaller centrifugal compressors have to be used in turbochargers to provide a higher boost pressure and extend the stable operating range. In many of these centrifugal compressors used for turbocharger applications, the tip clearance flow is the most significant source of loss and a major contributor to compressor instability. Tighter manufacturing tolerances have gone a long way to reduce tip clearances but there is a limit on how much this can be further reduced. Hence, designing the centrifugal compressor impellers with controlled tip clearance flow is a major requirement for developing high performance centrifugal compressors. However, before a design approach can be developed to reduce tip clearance flow, it is important to have a full understanding of the nature of clearance flow and how it interacts with the main flow.

There were a number of papers by Senoo and co-workers in the late 1980s and early 1990s to investigate the effect of tip clearance on centrifugal compressor performance. Senoo and Ishida [1, 2] developed a loss model for predicting the effect of tip clearance on impeller efficiency and pressure rise. Also Ishida et al. [3] investigated the effect of shaping the blade tips (e.g. rounded or sharp with endplates etc.) on

*Corresponding author (email: zxliu@tju.edu.cn)

the losses due to tip clearance. More recently Schleer et al. [4] investigated the effect of tip clearance on the onset of compressor instability by using a series of unsteady pressure transducers at the impeller tip. In addition, Schleer and Abhari [5] investigated the effect of the clearance flow on the flow field in the vaneless diffuser. Also Yamada, Eisenlohr, Krain et al. [6–9] investigated the effect of changing the number of blades on a transonic compressor impeller with splitter blades on the tip clearance flow field.

However, none of the above studies considered in detail the structure of the clearance flow in the impeller at various operating conditions both within the clearance region as well as how the clearance flow interacts with the main flow to create losses. This type of detailed study of the clearance flow is essential before one can develop a design methodology to reduce clearance losses. Detailed studies of tip clearance flow have been performed by Dambach et al. [10] for a large scale low speed radial-inflow turbine, by Yaras and Sjolander [11] for an axial flow turbine cascade and Storer and Cumpsty [12] on an axial compressor cascade. These investigations, which were mainly based on detailed experimental measurements at low speed with some feedback from early CFD computations with limited model of clearance flow (as in the case of Storer and Cumpsty), have provided important insights into the nature of clearance flow in these types of machines.

In the case of centrifugal compressor impellers, it is essential to understand the nature of clearance flow at high speed as the clearance flow plays an important role in the nature of the flow. Hence, an alternative approach is used, in which experimentally validated CFD computations are deployed to study the detailed nature of the clearance flow.

2 Test cases

The aim of this study is to use detailed computational flow prediction to better understand the nature of the clearance flow with the main flow in the impeller. In order to rely on the computational predictions it is essential to validate the predictions with detailed experimental measurements. For this purpose, a well-known test case with detailed measurements has been selected. The subsonic test case will be the Eckardt's radial impeller [13, 14] which has been widely used for validation of CFD prediction in centrifugal compressors. The measurements were made by LDV at DLR Cologne. The basic design conditions for a subsonic (Eckardt) impeller are shown in Table 1.

In order to predict the flow in the baseline impeller, the commercial CFD code CFX was used. In this case the final mesh size used for the study was based on a systematic mesh independency study.

An example of mesh independency study for the Eckardt impeller is shown in Figure 1. The coarse mesh has about 200 k cells for a single passage. The medium, fine and very fine meshes are 400, 800 and 1600 k cells, respectively. The parameter used for mesh independency is the clearance flow rate at design and off-design flow rates. The results indicate that the fine mesh which has 800 k cells already provides a mesh-independent solution and this mesh was then used for the rest of this study. The fine mesh distribution is 200×70×50 streamwise, spanwise and blade-blade, respectively. In this mesh 22 points are used in the tip gap region from blade tip to the casing and 20 points across the blade tip in the pitchwise direction. The value of Y^+ was found to be typically between 10 and 40 on all walls, which is appropriate for the standard wall function used in the CFD model.

The computational mesh used for the study is shown in Figure 2, together with the scaled-up of the mesh in the tip clearance area. The computational domain consists of an unshroud impeller followed by a vaneless diffuser. A frozen-rotor interface is used between the rotating and stationary components. The mesh has a structured H-O topology and consists of approximately 800 k nodes. The computations were performed with the nominal clearances as shown in Table 1. Additional computations were performed with zero tip clearance with the shroud stationary so that the scraping effect could be modeled. In addition, computations were performed with tip clearance of 0.754 and 1.29 mm. The first clearance corresponds to 2.9% of exit blade height and 0.9% of inlet blade height while the second tip clearance corresponds to 4.96% of exit blade height and 1.6% of

Table 1 Subsonic compressor design parameters

Item	Value
Shaft speed (rpm)	14000
Design mass flow rate (kg/s)	5.31
Impeller tip clearance (mm)	200
Rotor tip speed (m/s)	293
Pressure ratio	2.1
Blade number	20
Nominal tip clearance (mm)	0.0
Additional clearances (mm)	0.754, 1.29

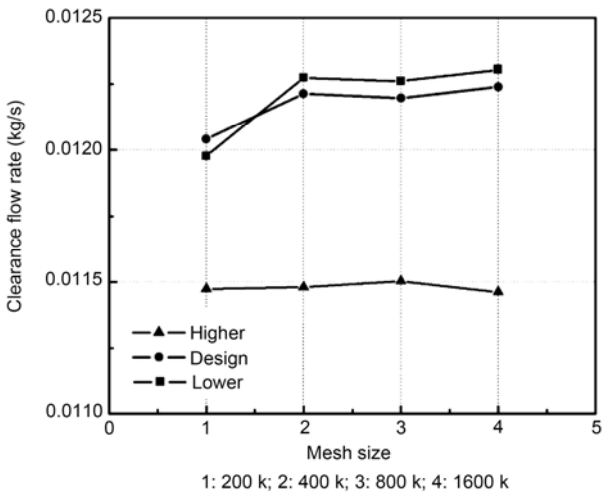

Figure 1 Mesh independency study for Eckardt Impeller.

inlet blade height. The different clearances were implemented by maintaining the same casing shape and cutting the impeller blade tip. For flow analysis, compressible RANS equations and k-ε turbulence model were used. Computations were performed at various flow rates at 14000 rpm. Three flow rates were calculated for detailed analysis. Design flow rate is 5.31 kg/s, under which the LDV measurement was made. This will be referred to as 'Design' in figures and legends and corresponds to a flow coefficient of 0.12. Flow rate of 3.40 kg/s corresponding to flow coefficient of 0.076 is labeled as 'Lower' in legends and finally the flow rate of 7.11 kg/s, corresponding to flow coefficient of 0.168, is labeled as 'Higher' in the graphs.

The predicted flow field is compared with the LDV measurement of Eckardt (1976) in Figure 3. The comparison is made at 14000 rpm and design flow rate of 5.31 kg/s.

Figure 3 shows the comparison of the spanwise and pitchwise variations in relative velocity at Plane I (M=0.08), Plane III (M=0.59) and Plane V (M=1.01), where M represents the meridional direction location of the impeller, with a dimensionless value between 0.0 and 1.2. The CFD predictions generally correlate well with the LDV measurement at all three locations and hence these data can be used to explore the flow in the tip clearance region in details.

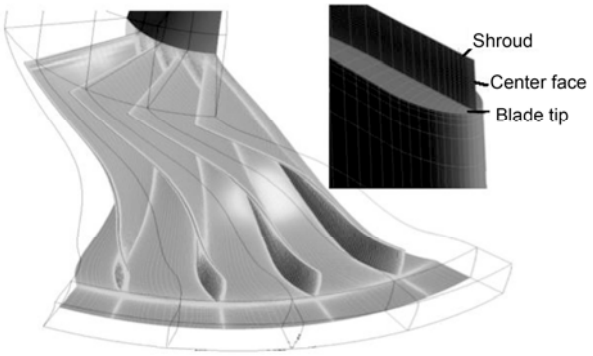

Figure 2 Computational mesh for Eckardt impeller.

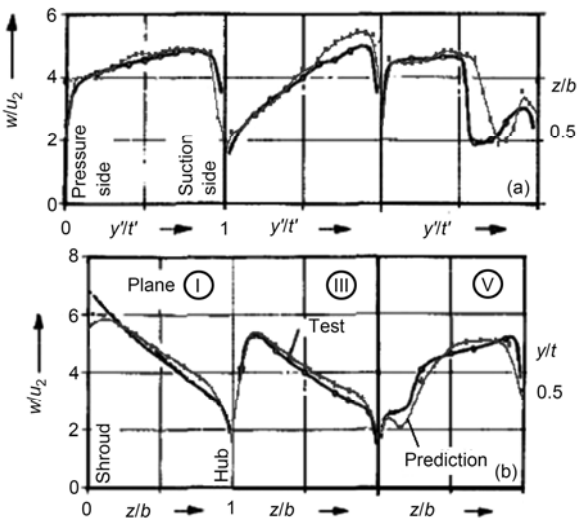

Figure 3 Comparison of prediction and measurement. (a) Spanwise flow variation; (b) pitchwise flow variation.

3 Nature of tip clearance flow in impeller

3.1 General observations and underlying factors affecting the clearance flow

In Figure 4(a), the variations of isentropic efficiency at the impeller exit with different flow rates for several tip clearances are compared. The efficiency drops for different flow rates are shown in Figure 4(b). Here, the clearances of 0.754 and 1.29 mm correspond to 2.9% and 4.96% of the exit blade height, respectively, calculated by the formula 100 $\times t/b_2$, where t is the value of tip clearance and b_2 is the exit blade height. The results confirm that there is a significant drop in efficiency of about 2.6% between zero tip clearance case and the case with a clearance of 0.754 mm (2.9%) at the near peak efficiency condition. The drop in efficiency is even more significant for a 4.96% tip clearance, approaching 3.5% at a higher flow rate. The loss of efficiency between 0.754 and 1.29 mm (i.e. almost doubling of clearance from 2.9% to 4.96%) is less than one percent. In-

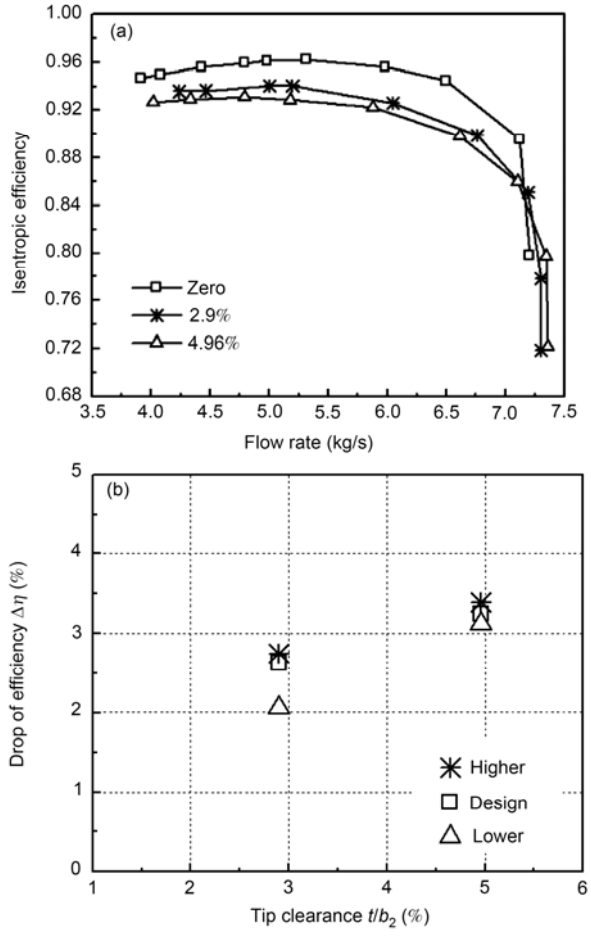

Figure 4 Effect of tip clearance on impeller performance. (a) Impeller efficiency; (b) efficiency drop.

creasing the tip clearance, as expected, would result in a slight increase of the impeller choke flow rate.

The variation in clearance flow rate (identified as $Q_{l)}$ through tip gap as a percentage of total impeller flow rate (identified as Q_{in}) at various impeller flow rates and for different tip clearances are shown in Figure 5. These were computed by summing the flow rate through the clearance area at the tip. Since the main source of loss due to tip clearance is due to the mixing of the clearance flow on the suction surface with the main flow, the higher the total amount of clearance flow rate the higher the associated losses due to tip clearance. According to the results shown in Figure 5, the clearance flow rate peaks at around flow rate of 4.5 kg/s that is close to the design point/peak efficiency point. However, the amount of clearance flow rate drops off rapidly at high flow rates close to choke and at low flow rates close to stall. The reason for this drop in flow rate at off-design conditions needs to be investigated by looking more closely at the main driving forces of clearance flow.

The clearance flow has a major effect on the blade pressure distribution. This can be seen clearly in Figure 6, where the blade surface pressure distribution at design flow rate is shown at 95% span with different tip clearances. The clearance flow seems to have little effect on blade loading between leading edge and 50% meridional chord. However, from 50% chord to the trailing edge significant drop in static pressure on the pressure surface can be observed. This region in fact corresponds to relatively high values of leakage flow rate.

The static pressure on suction surface, however, is generally unchanged until about 70% of chord where a significant drop starts to be observed and then increases until the trailing edge. Almost doubling the clearance gap from 0.754 to 1.29 mm does not have a significant effect on the surface pressure distribution. However, the 1.29 mm clearance which corresponds to 4.96% of exit blade width shows a more dramatic drop on pressure surface near the trailing edge.

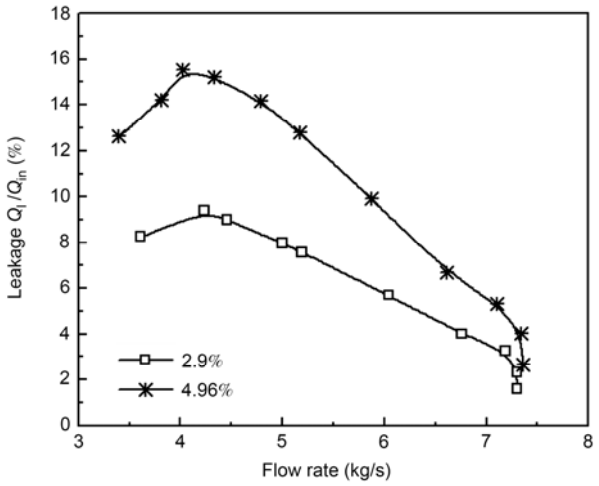

Figure 5 Effect of tip clearance on clearance leakage.

The effect of clearance flow on surface pressure at 95% span at the flow lower than the design flow, as shown in Figure 7(a), is in fact similar to that at the design flow. At a higher than design flow (Figure 7(b)) the effect is more pronounced, with significant drops in surface pressure on both suction and pressure surfaces from 40% of meridional chord. The effect is further complicated by the presence of a shock in the inducer at the high flow rate. The changes in

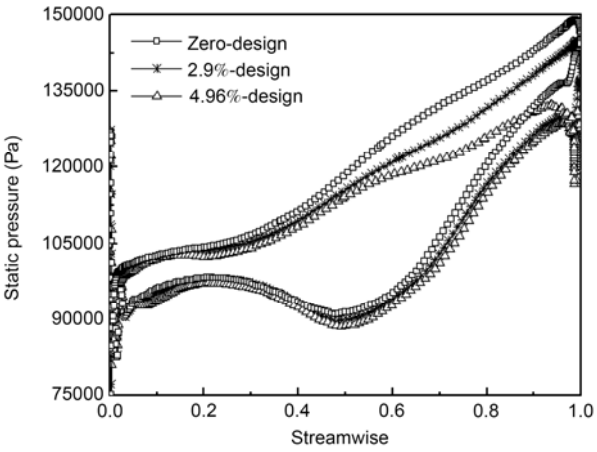

Figure 6 Effect of tip clearance on blade surface pressure.

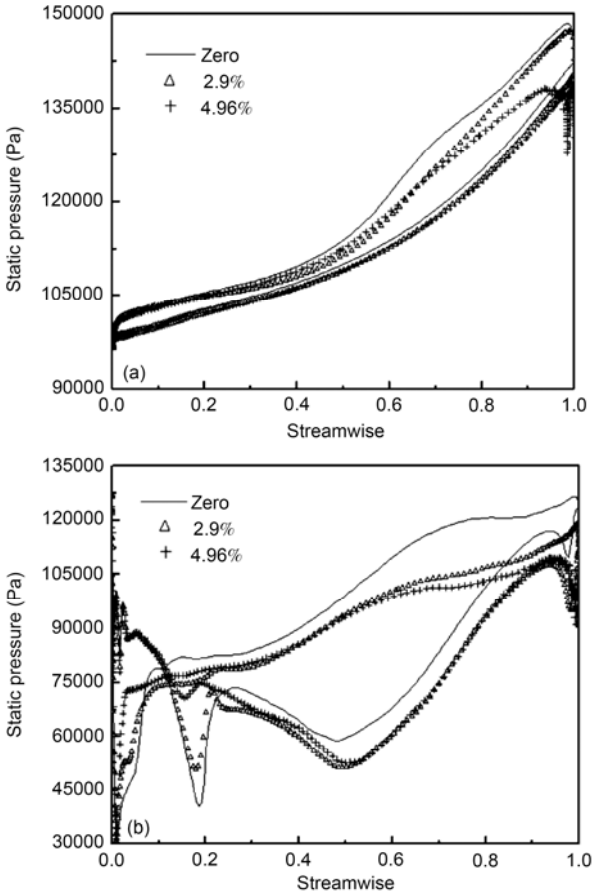

Figure 7 Effect of tip clearance on blade surface pressure. (a) Lower than design flow rate; (b) higher than design flow rate.

clearance affect the shock formed in the inducer. The main driving force for clearance flow is the blade loading, which is the difference in blade surface pressure between pressure and suction surfaces at the tip.

In Figure 8, the effect of tip clearance on the streamwise variation of blade loading at 95% span is plotted. The blade loading is obtained from the difference between the static pressure on the pressure (P_p) and suction surface (P_s) of the blade normalized by the inlet dynamic head (P_{din}). The abscissa is the meridional distance from the leading edge normalized by the total meridional length at 95% span. Broadly speaking, even at 95% span, the tip clearance does not change the overall shape of the blade loading at zero clearance.

In Figure 9(a), the blade loading distribution is shown for the flow rates of design, lower than and higher than the design flow rate for a tip clearance of 0.754. In Figure 9(b), the streamwise variation in leakage flow rate normalized by the inlet average flux of impeller is shown at the design, lower and higher flow rates. The streamwise variation in leakage flow correlates strongly with the blade loading, the regions of high and low blade loading are directly associated with high and low leakage flows, respectively. The negative loading for the first 20% at the high flow rate due to incidence effect in fact results in a reversal of the direction of clearance flow. This issue will be discussed later in detail. A very similar correlation between ΔP and leakage flow rate can be also seen at 1.29 mm clearance.

3.2 Flow field in the tip gap

In order to understand the nature of the flow in the tip gap, the detailed flow field through the tip gap with 0.754 and 1.29 mm clearances were obtained from the CFD solution at meridional distances of 25%, 50%, 75% and 90%. The results are presented in Figures 10 and 11 in terms of streamline plots. The results indicate the presence of a small recirculation region at the tip of the pressure side, especially

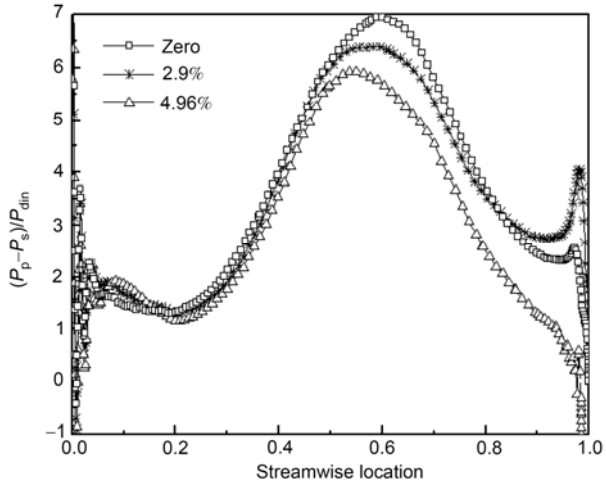

Figure 8 Effect of tip clearance on blade loading.

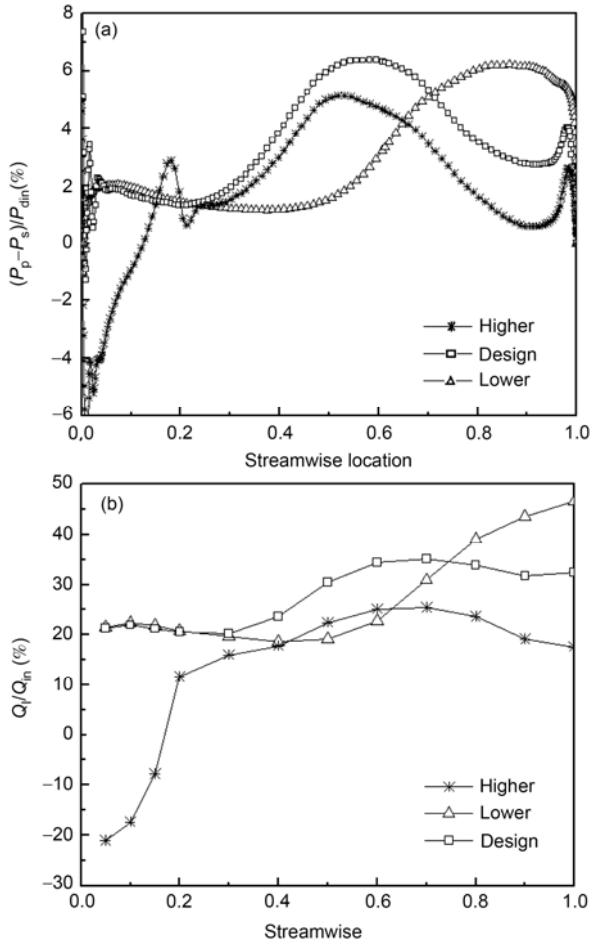

Figure 9 Correlation between (a) blade loading and (b) leakage flow.

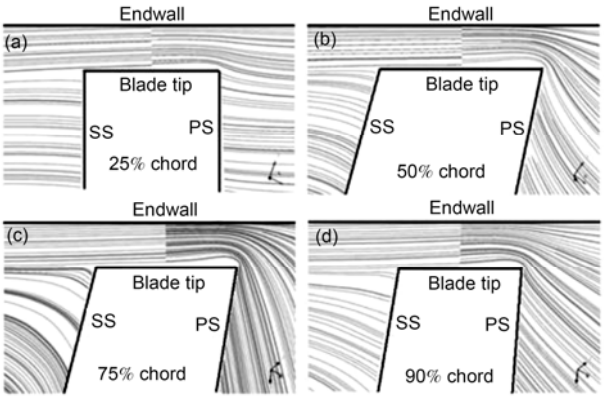

Figure 10 Predicted streamline patterns in the tip gap with 0.754 mm clearance at design flow. (a) 25% chord; (b) 50% chord; (c) 75% chord; (d) 90% chord.

at meridional chords of 50%, 75% and 90%. In fact, the separation area is visible at 75% meridional chord and not easy observed at 50% and 90% locations. So, two partially enlarged pictures corresponding to the box position labeled as "*A*" and "*B*" follow and clearly show the flow separation. Also of interest is the trajectory of the streamlines entering

the tip gap at different streamwise positions. At the 25% location of the streamwise line, the streamlines enter the gap with little change along the spanwise direction. At 50% and 75% of the chord, the flow enters the gap from further down the blade span, indicating very strong acceleration of the gap flow in this region, which explains the drop in the pressure side static pressure at the tip, as observed in Figures 6 and 7. Note the discontinuous streamlines in the middle of the gap is caused by the direction computation from the grid, which happens to be the interface of the pressure side and the suction side.

In order to better understand the nature of the flow in the tip gap, spanwise variation of relative flow angle across the gap at the above 4 streamwise locations were obtained and are presented in Figure 12 at locations close to pressure side (10%) and suction side (100%). The flow angle is defined as $\tan^{-1}(W_\omega/W_m)$, where W_ω is the relative velocity component of the rotating direction, and W_m is the relative velocity component of the meridional direction. The longitudinal axis is dimensionless gap position. The results indicate that the flow into the gap from pressure side is almost tangential from 50% to 90% chord for most of the gap apart from the shear layer for the first 20% across the blade tip where significant streamwise component exists. At 25% chord, however, the flow angles have a significant streamwise component for most of the gap apart from the last 20% close to the endwall. At the suction side (100% location) at 50% chord the flow is almost tangential. But at 25% chord the flow angle leaving over the blade tip is 30° as opposed to a flow angle of 52° on the suction surface of the blade at 85% span. At 75% chord, the flow leaving over the blade tip is at 65° while at the same location at 85% span on suction surface of blade the flow angle is 4.5°.

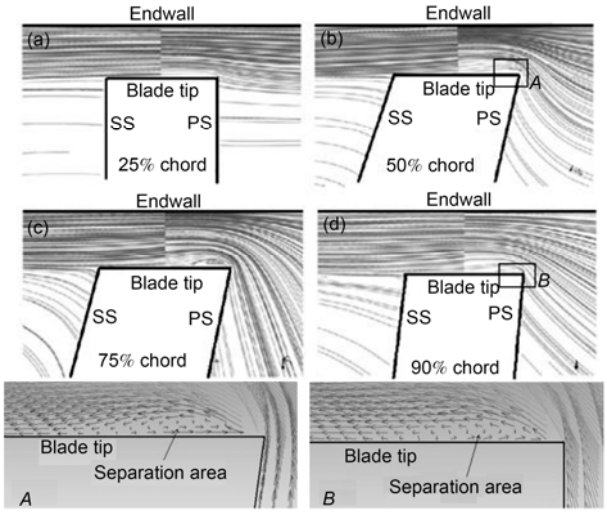

Figure 11 Predicted streamline patterns in the tip gap with 1.29 mm clearance at design flow. (a) 25% chord; (b) 50% chord; (c) 75% chord; (d) 90% chord.

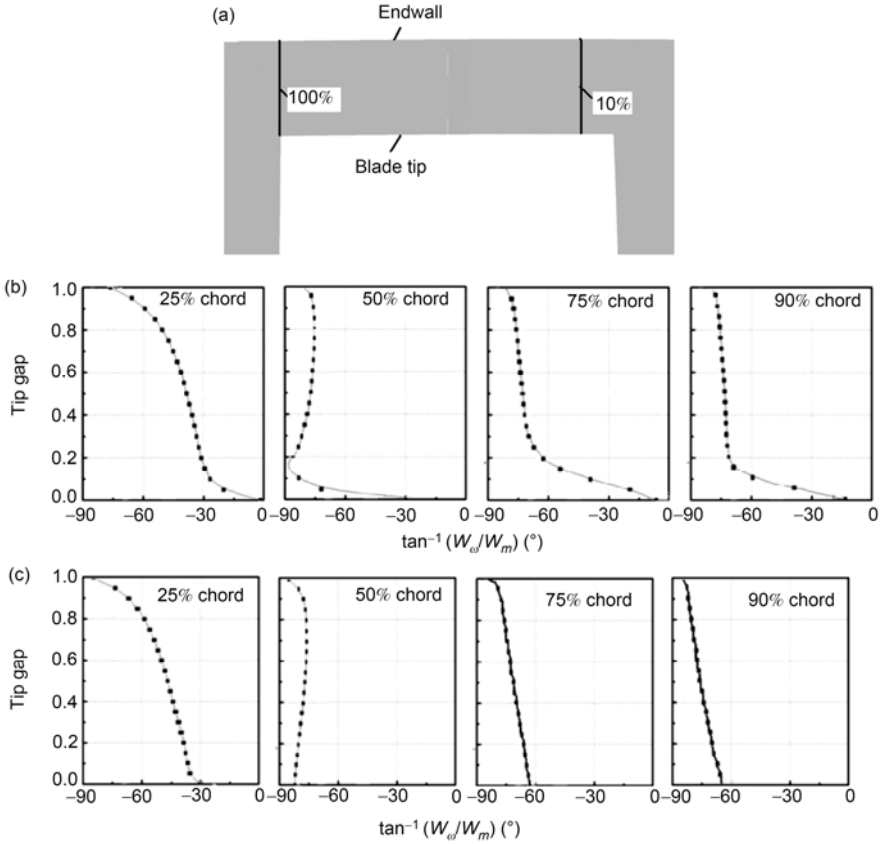

Figure 12 (a) Variation of flow angles into (10%) and out (100%) of the tip gap at design flow: 0.754 mm tip clearance; (b) pressure side: 10% gap location; (c) suction side: 100% gap location.

In Figure 13 the variations of entropies at 10% and 100% gap locations are presented at various streamwise locations. The results generally confirm that most of the loss is generated in the shear layer covering the first 20% of gap height over the blade at 10% location. The losses seem to be most significant at 50% chord and 75% chord locations. But overall, the average entropy at 100% location leaving the gap is at a similar level to that at 10% location, confirming that in fact little loss is generated in the gap itself.

3.3 Interaction of tip gap flow with suction side main flow

In order to understand the nature of loss generation by the interaction of the clearance flow and the main flow, the flow predictions were processed to locate the clearance vortex. The resulting plots are shown in Figure 14 at the design flow rate for 2.9% and 4.96%. The trajectory of the clearance flow changes significantly between 2.9% and 4.96% clearances but generally there is a close correlation between the vortex core and high loss in the inducer at design flow.

The trajectory of the tip leakage vortex at higher flow condition is shown in Figure 15 at 2.9% and 4.96% clearances. The results indicate that at this flow rate, two sets of vortices are generated, one starting from close to the leading edge on the pressure surface and another further downstream on the suctions surface. This may seem surprising. However, it is seen from Figure 9(a) that at high flow rates, the blade loading is negative because of incidence effect and in fact the leakage flow (Figure 9(b)) is also negative for the first 20% of meridional chord. It means that the leakage flow in fact moves from the suction to the pressure surface and hence a clearance vortex is generated from the pressure surface.

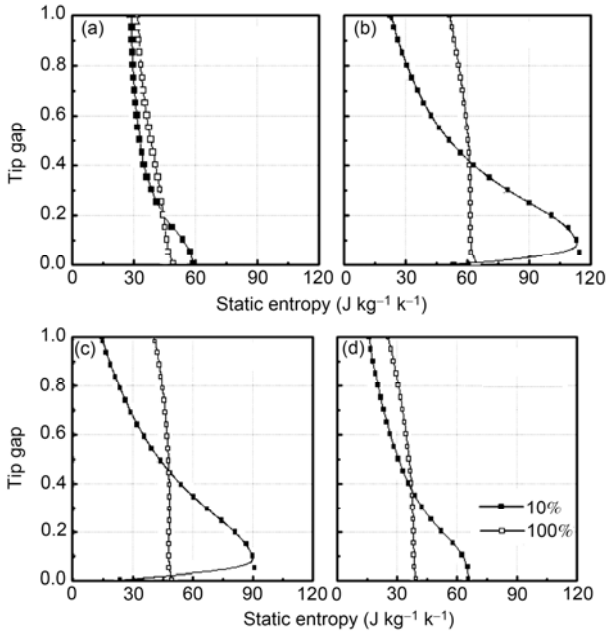

Figure 13 Variations of entropy into (10%) and out (100%) of the tip gap at design flow: 0.754 mm tip clearance. (a) 25% chord; (b) 50% chord; (c) 75% chord; (d) 90% chord.

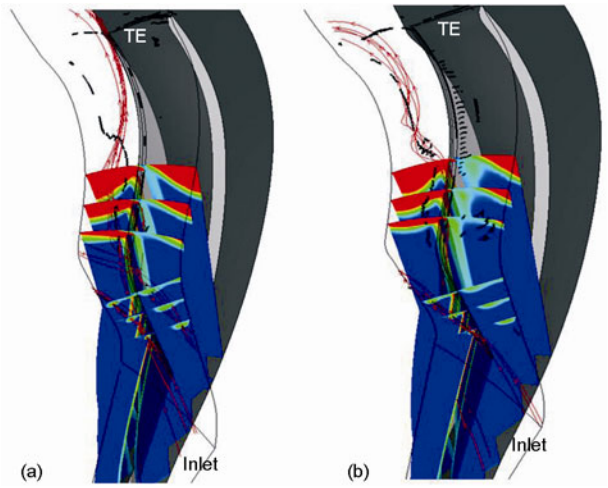

Figure 14 Clearance vortex trajectory-design flow. (a) 2.9% clearance; (b) 4.96% clearance.

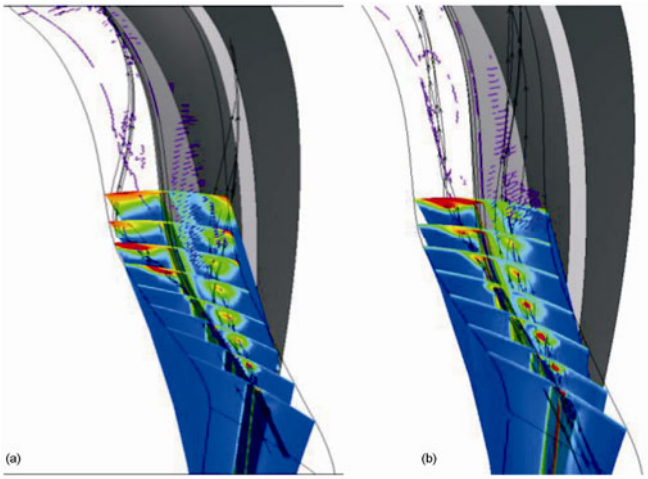

Figure 15 Clearance vortex trajectory-higher flow. (a) 2.9% clearance; (b) 4.96% clearance.

4 Conclusions

CFD predictions for flow through Eckardt impeller validated by LDV measurements were used to investigate the detailed nature of the clearance flow in a subsonic impeller. The flow through the impeller was calculated at zero clearance, at a clearance of 2.9% of exit width and clearance of 4.96% of exit width. The CFD predictions for Eckardt impeller show higher change in blade surface static pressure with increasing tip gap from zero clearance. By comparison, a very close correlation between the blade loading (jump in static pressure across the blade) and the leakage flow distribution along the streamwise is found. Also, increasing the

clearance gap does not seem to broadly change the shape of the blade loading curve in the zero tip clearance case, although the value of the blade loading is reduced, especially from 50% chord to the trailing edge. Streamlines trajectory of the tip leakage flow shows very strong streamline acceleration into the gap, especially at 50% and 75% of meridional chord. Variation of spanwise flow angle across the gap at the entry and exit from the tip gap indicates the flow into and out of the gap has significant streamwise component at 25% chord but is essentially tangential at 50%, 75% and 90% of meridional chord. Variation of spanwise entropy at the entry and exit from the tip gap indicates there is very little loss inside the tip gap. However, a shear layer with relatively high entropy can be observed over the gap at entries of 50%, 75% and 90% meridional chord. Identification of the clearance vortex core confirms that the clearance vortex is a major source of loss. Also the results confirm the presence of a second clearance vortex at high flow rates because of a negative incidence, resulting in movement of clearance flow from suction side to pressure side in the first 20% of meridional chord.

This work was supported by the National Natural Science Foundation of China (Grant No. 51276125) and the National Basic Research Program of China ("973" Project) (Grant No. 2012CB720101).

1 Senoo Y, Ishida M. Pressure loss due to the tip clearance of impeller blades in centrifugal and axial blowers. J Eng Gas Turb Power, 1986, 108: 32–37
2 Senoo Y, Ishida M. Deterioration of compressor performance due to tip clearance of centrifugal impellers. J Turbomach, 1987, 109: 55–61
3 Ishida M, Ueki H, Senoo Y. Effect of blade tip configuration on tip clearance loss of a centrifugal impeller. J Turbomach, 1990, 112: 14–18
4 Schleer M, Song S J, Abhari R S. Clearance effects on the onset of instability in a centrifugal compressor. J Turbomach, 2008, 130: 031002-1
5 Schleer M, Abhari R. Clearance effects on the evolution of the flow in the vaneless diffuser of a centrifugal compressor at part load conditions. J Turbomach, 2008, 130: 031009
6 Yamada K, Tamagawa H, Ibaraki S, et al. Comparative study on tip clearance flow fields in two types of transonic centrifugal compressor impeller with splitter blades. In: ASME Turbo Expo 2010: Power for Land, Sea and Air. ASME Paper GT2010-23345, 2010
7 Eisenlohr G, Krain H, Richter F, et al. Investigations of the flow through a high pressure ratio centrifugal impeller. In: ASME Turbo Expo 2002: Power for Land, Sea and Air. ASME Paper GT-2002-30394, 2002
8 Krain H, Hofmann B. Flow physics in high pressure centrifugal compressors. In: ASME Turbo Expo 1998: Power for Land, Sea and Air. ASME FEDSM98-4853, 1998
9 Krain H, Hoffmann B, Rohne K H, et al. Improved high pressure ratio centrifugal compressor. In: ASME Turbo Expo 2007: Power for Land, Sea and Air. ASME Paper GT2007-27100, 2007
10 Dambach R, Hodson H P, Hunstman I. An experimental study of tip clearance flow in a radial inflow turbine. In: ASME Turbo Expo 1998: Power for Land, Sea and Air. ASME Paper 98-GT-467, 1998
11 Yaras M I, Sjolander S A. Effect of simulated rotation on tip leakage in a planar cascade of turbine blades: Part 1-tip gap flow. J Turbomach, 1992, 114: 652–659
12 Storer J A, Cumpsty N A. Tip leakage flow in axial compressors. J Turbomach, 1991, 113: 252–259
13 Eckardt D. Instantaneous measurements in the jet-wake discharge flow of a centrifugal compressor impeller. J Eng Power ASME, 1975, 97: 337–349
14 Eckardt D. Detailed flow investigation within a high speed centrifugal compressor impeller. J Fluid Eng ASME, 1976, 98: 390–405